Experimental Hematology

Experimental Hematology 2016;44:247–256

Erythroblast enucleation is a dynein-dependent process

Isuzu Kobayashi[a], Kumi Ubukawa[a], Kotomi Sugawara[b], Ken Asanuma[c], Yong-Mei Guo[a], Junsuke Yamashita[c], Naoto Takahashi[a], Kenichi Sawada[d], and Wataru Nunomura[e,f]

[a]*Department of Hematology, Nephrology, and Rheumatology, Graduate School of Medicine, Akita University, Akita, Japan;* [b]*Department of Hematology, Nephrology, and Rheumatology, Master Course of Graduate School of Medicine, Akita University, Akita, Japan;* [c]*Center for Radio Isotope, Akita University, Akita, Japan;* [d]*Akita University, Akita, Japan;* [e]*Research Center for Science, Graduate School of Engineering and Resource Science, Akita University, Akita, Japan;* [f]*Department of Life Science, Graduate School of Engineering and Resource Science, Akita University, Akita, Japan*

(Received 25 August 2015; revised 14 December 2015; accepted 17 December 2015)

Mammalian erythroblasts undergo enucleation through a process thought to be similar to cytokinesis. Microtubule-organizing centers (MTOCs) mediate organization of the mitotic spindle apparatus that separates the chromosomes during mitosis and are known to be crucial for proper cytokinesis. However, the role of MTOCs in erythroblast enucleation remains unknown. We therefore investigated the effect of various MTOC inhibitors on cytokinesis and enucleation using human colony-forming units–erythroid (CFU-Es) and mature erythroblasts generated from purified CD34$^+$ cells. We found that erythro-9-[3-(2-hydroxynonyl)]adenine (EHNA), a dynein inhibitor, and monastrol, a kinesin Eg5 inhibitor, as well as various inhibitors of MTOC regulators, including ON-01910 (Plk-1), MLN8237 (aurora A), hesperadin (aurora B), and LY294002 (PI3K), all inhibited CFU-E cytokinesis. Among these inhibitors, however, only EHNA blocked enucleation. Moreover, terminally differentiated erythroblasts expressed only dynein; little or none of the other tested proteins was detected. Over the course of the terminal differentiation of human erythroblasts, the fraction of cells with nuclei at the cell center declined, whereas the fraction of polarized cells, with nuclei shifted to a position near the plasma membrane, increased. Dynein inhibition impaired nuclear polarization, thereby blocking enucleation. These data indicate that dynein plays an essential role not only in cytokinesis but also in enucleation. We therefore conclude that human erythroblast enucleation is a process largely independent of MTOCs, but dependent on dynein.

Mammalian erythropoiesis culminates in enucleation, an incompletely understood process entailing the expulsion of the nucleus from the cytoplasm of erythroblasts. During erythropoiesis, stem cells undergo lineage-specific commitment and generate erythroid progenitor cells through cellular division events that include both nuclear (mitosis) and cytoplasmic (cytokinesis) division. These progenitor cells consist of burst-forming units–erythroid (BFU-Es) and their progeny, colony-forming units–erythroid (CFU-Es) [1–4]. Then over an additional 6 to 7 days, the CFU-Es proliferate and differentiate into mature erythroblasts [1,5]. During terminal differentiation, mammalian erythroblasts undergo enucleation, becoming reticulocytes and, subsequently, mature erythrocytes. The expelled nuclei are phagocytosed by reticular cells such as macrophages (for a review, see [6]).

The process of enucleation is thought to be similar to cytokinesis, and many of the general principles of cytokinesis apply to enucleation. In both cytokinesis and enucleation, the cytoskeleton is key in the choice and positioning of the division site. Once this site is chosen, there is local assembly of a contractile actomyosin ring, during which nonmuscle myosin IIB remodels the plasma membrane [5]. Trafficking of the necessary components to the division site and membrane fusion lead to the physical separation of the daughter cells (for a review, see [7,8]). Wang et al.

Offprint requests to: Wataru Nunomura, Department of Life Science, Graduate School of Engineering and Resource Science, Akita University, Tegata-Gakuên 1-1, Akita 010-8502, Japan; E-mail: nunomura@gipc.akita-u.ac.jp

Supplementary data related to this article can be found online at http://dx.doi.org/10.1016/j.exphem.2015.12.003.

http://dx.doi.org/10.1016/j.exphem.2015.12.003

reported that nuclear polarization regulated by phosphoinositide 3-kinase (PI3K) is important for the enucleation [9]. During polarization, the nucleus becomes displaced to one side of the cell, near the plasma membrane, while actin becomes restricted to the other side, where dynamic cytoplasmic contractions generate pressure that pushes the viscoelastic nucleus through a narrow constriction in the cell surface, forming a bud. These findings implicate PI3K and its products in the polarization and enucleation of erythroblasts [9].

Microtubule-organizing centers (MTOCs) function as sites where microtubule formation begins, as well as locations where free ends of microtubules are attracted to proteins anchored in the cytoplasmic membrane [10]. The most notable MTOCs are the centrosomes formed during interphase and the mitotic spindle poles. Thus, MTOCs are essential for proper cytokinesis. The degree to which MTOCs contribute to the enucleation of terminally differentiated erythroblasts remains unknown, however. γ-Tubulin is a member of the tubulin family and is important for nucleation and polar orientation of microtubules [10,11]. γ-Tubulin is an abundant component of centrosomes and spindle pole bodies, where it is found within γ-tubulin ring complexes, which chemically mimic the plus end of microtubules, thus enabling microtubules to bind [12,13]. Another molecule, the motor protein dynein, mediates unidirectional movement toward MTOCs (minus end of microtubules), whereas kinesins "walk" along microtubule filaments toward the plus end, often enabling transport of cargo from the cell center toward the periphery [14–16]. The motor functions of both dynein and kinesins are known to support cytokinesis, but their roles in erythroblast enucleation remain unclear [17–19].

In the present study, therefore, we investigated the contributions made by dynein, kinesin, Eg5, and several MTOC regulatory proteins to the process of human erythroblast enucleation. Here we illustrate that although the motor proteins dynein and Eg5 and the various MTOC regulatory proteins tested were all needed for CFU-E cytokinesis (proliferation), only dynein was necessary for the cell division and nuclear polarization during terminal erythroblast differentiation and enucleation. Enucleation is thus independent of most MTOC-related proteins, but dependent on dynein.

Methods

Cell preparations

Granulocyte colony-stimulating factor (G-CSF)-mobilized human peripheral blood $CD34^+$ cells were purified from healthy volunteers as described previously and stored in liquid nitrogen until required. Informed consent was obtained from all subjects prior to their entry into this study, and the study was pre-approved by the Akita University Graduate School of Medicine Committee for the Protection of Human Subjects [2].

To generate erythroid progenitor cells, $CD34^+$ cells were thawed and prepared for culture as previously described [2]. Cells were cultured in Iscove's modified Eagle's medium (IMDM), erythroid medium containing 20% fetal calf serum (FCS), 10% heat-inactivated pooled human AB serum, 1% bovine serum albumin (BSA), 10 μg/mL insulin, 0.5 μg/mL vitamin B_{12}, 15 μg/mL folic acid, 50 nmol/L β-mercaptoethanol (β-ME), 50 U/mL penicillin, and 50 μg/mL streptomycin in the presence of 50 ng/mL interleukin (IL)-3, 50 ng/mL stem cell factor (SCF), and 2 IU/mL erythropoietin (EPO). Cells were maintained at 37°C in a 5% CO_2 incubator. On day 7 of culture (D7), the cells were harvested and washed three times with IMDM containing 0.1% BSA and stored at 4°C until required. The maturation level of the D7 cells was similar to that of CFU-Es, as reported elsewhere [2,3]. Hereafter, D7 cells will be referred to as CFU-Es. Because the cells were not completely synchronized, the effects of inhibitors on cell proliferation and the enucleation ratio (describe in the Supplementary Methods, online only, available at www.exphem.org) were decided after incubation for 24 h.

Aliquots of CFU-Es were then cultured in erythroid medium with EPO alone, without β-mercaptoethanol, SCF, or IL-3 to induce differentiation with or without various the inhibitors of cell division. The volume of inhibitor and control solutions (H_2O or dimethyl sulfoxide [DMSO]) was fixed at 5% of the erythroid medium. The final concentration of DMSO in the erythroid medium was 0.1% (v/v), as higher concentrations are toxic to human erythroid progenitors. The cells were harvested at various times, washed three times with IMDM containing 0.1% BSA, resuspended in IMDM containing 0.1% BSA, and stored at 4°C until required.

Morphologic and immunochemical analysis of cells cultured with and without inhibitors

The cells were classified based on the whether the nucleus was localized at the center of the cells (centered); the cells were spherical containing a condensed nucleus located to one side, close to the plasma membrane (polarized); or the cells were enucleated (reticulocytes). Other cell types, such as multinucleate cells and cells with condensed apoptotic nuclei, were classified as "other." Images of cells classified as described are provided in Supplementary Figure E1 (online only, available at www.exphem.org). The fractions of each cell type were calculated as described in the previous section. Results are presented as the means ± SD of three independent experiments.

Immunochemical distributions of γ-tubulin and dynein were determined using confocal microscopy as described above. D10 cells were cultured in the presence or absence of 400 μmol/L erythro-9-[3-(2-hydroxynonyl)]adenine (EHNA).

Other information

Additional methods and details of are described in the Supplementary Methods.

Results

Dynein inhibitor blocks division of CFU-Es

We first examined the effects of inhibitors of cell division on primary human CFU-Es generated from purified $CD34^+$ cells. Given that cellular division consists of both

mitotic and cytokinetic events and inhibition of either step should block cell proliferation, effective inhibitors were defined as those that blocked CFU-E proliferation.

Figure 1A and B illustrates total cell numbers and morphology when human CFU-Es were cultured without inhibitors. EHNA, a specific inhibitor of dynein ATPase activity, completely blocked cell proliferation (Fig. 1C). Among the cells incubated with a motor protein inhibitor, the fraction of cells in G1/G0/S phase (46.0 ± 0.6% for EHNA, as illustrated in Fig. 1D) was little changed from control, though there was a significant reduction in the mitotic fraction (4*n*<). The morphology of the EHNA-treated cells was similar to that of control cells at 0 hours (Fig. 1E). No multinucleate cells were observed among the cells incubated with 400 μmol/L EHNA. To avoid the possibility of a nonspecific effect of EHNA on the proliferation of CFU-Es, dynein and α-tubulin expression was analyzed using Western blotting (Supplementary Figure E2, all supplementary figures are online only, available at www.exphem.org), whereas expression of CD71 and glycophorin A (GPA) was analyzed using fluorescence-activated cell sorting (FACS) (Supplementary Figure E3). There was no nonspecific effect on the expression of dynein or α-tubulin. The levels of CD71 and GPA expression indicated that EHNA inhibited cell proliferation. We also examined the effect of EHNA on gene expression of GATA1 and GLUT1 (Supplementary Figure E4), but found no significant changes in cells cultured with or without EHNA for 24 h. Mitotic kinesin Eg5, serving as a control motor protein moving in the opposite direction of dynein, was blocked by monastrol, which was previously reported to affect cell proliferation [5,20,21]. Our present findings confirm those earlier results (Supplementary Figure E5A–C). Or results also indicate that EHNA selectively inhibits dynein with no nonspecific effects. No multinucleate cells were observed after treatment with high concentrations of EHNA, which indicates that EHNA does not affect actin polymerization. Thus, EHNA specifically blocks human CFU-E proliferation as effectively as monastrol [5].

Inhibition of MTOC regulators blocks CFU-E proliferation

ON-01910, an inhibitor of Plk1, which is an early trigger for G2/M transition; MLN8237, an inhibitor of aurora A, which is associated with centrosome maturation and separation and, thus, regulates spindle assembly and stability; and hesperadin, an inhibitor of aurora B, which functions in the attachment of the mitotic spindle to the centromere all completely blocked CFU-E proliferation (Fig. 2A). Cell cycle analysis revealed that ON-01910 reduced the cell fraction in G1/G0 phase, leading to accumulation of cells in S (13.7 ± 1.9%) and G2/M (24.7 ± 1.9%) phases, and dramatically increased the dead cell fraction (32.8 ± 3.2%) (Fig. 2B). Many CFU-Es treated with ON-01910 for 48 hours exhibited nuclear fragmentation characteristic of early apoptosis (Fig. 2C). Treatment with MLN8237 also significantly reduced the cell fraction in G1/G0 phase (35.4 ± 1.3%), resulting in the accumulation

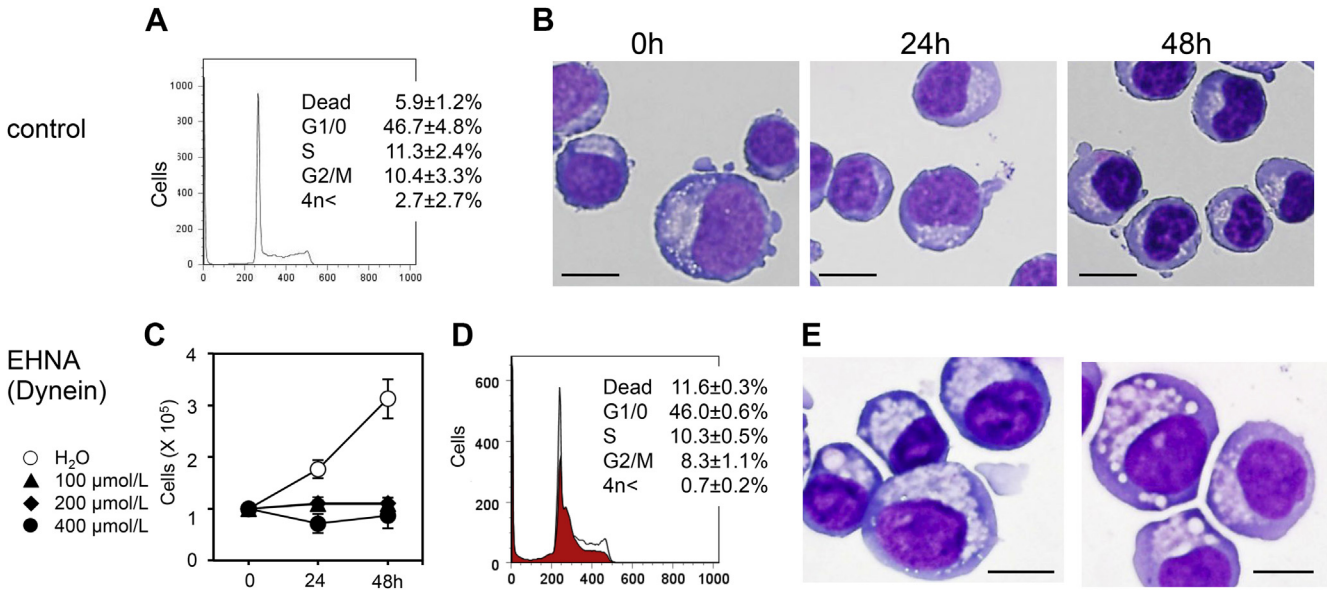

Figure 1. Dynein inhibitor blocks CFU-E proliferation. Human D7 CFU-Es generated from purified $CD34^+$ cells were cultured for the indicated periods in the presence of EPO with or without the dynein inhibitor EHNA. (**A**) Cell cycle analysis of D7 cells without inhibitors. (**B**) May–Grünwald–Giemsa staining of D7 cells after culture for 0, 24, or 48 hours without inhibitors. (**C**) Effects of the indicated concentrations of inhibitors or vehicle on CFU-E proliferation. Results are presented as the means ± SD of three independent experiments. (**D**) Cell cycle analysis of D8 cells after culture for 24 hours with (*red areas*) or without (*solid lines*) 400 μmol/L EHNA. A representative result from three independent experiments is presented as the mean ± SD. (**E**) May–Grünwald–Giemsa staining of D8–D9 cells after culture for 24 or 48 hours with or without 400 μmol/L EHNA. A representative result from three independent experiments is shown. Note that no multinucleate cells were found among those incubated with 400 μmol/L EHNA. The results indicated that EHNA did not have effects on actin. Bar = 10 μm.

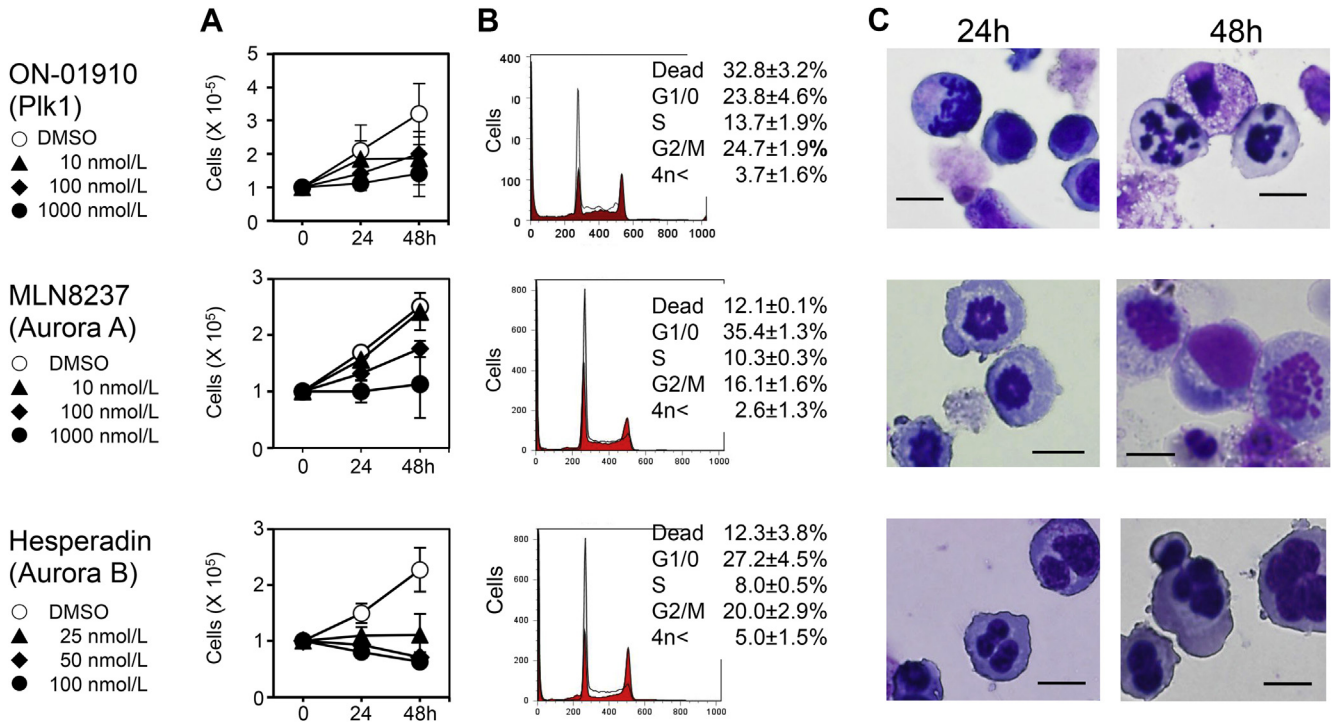

Figure 2. Inhibition of MTOC regulators blocks CFU-E proliferation. Human D7 CFU-Es were cultured for the indicated periods in the presence of EPO with or without inhibitors of Plk1 (ON-01910), aurora A (MLN8237) and aurora B (hesperadin). (**A**) Effects of the indicated concentrations of inhibitor or vehicle on CFU-E proliferation. Results presented are the means ± SD of three independent experiments. (**B**) Cell cycle analysis of D8 cells after culture for 24 hours with (*red areas*) 1,000 nmol/L ON-01910, 1,000 nmol/L MLN8237, or 100 nmol/L hesperadin. A representative result from among three independent experiments is presented as the mean ± SD. (**C**) May–Grünwald–Giemsa staining of D8–D9 cells after culture for 24 or 48 hours with or without 1,000 nmol/L ON-01910, 1,000 nmol/L MLN8237, or 100 nmol/L hesperadin. A representative result from three independent experiments is shown. Bar = 10 μm.

of cells in G2/M phase and an increase in dead cells (Fig. 2B). Hesperadin treatment led to an even greater reduction in G1/G0 cells (27.2 ± 4.5%) and a corresponding increase in G2/M cells (20.0 ± 2.9%). Abnormally shaped nuclei and multinuclear cells also appeared among hesperadin-treated CFU-Es (Fig. 2C). Consistent with earlier reports, we found that the phosphoinositide 3-kinase (PI3K) inhibitor LY294002 blocks CFU-E proliferation with an increase in the dead cell fraction (10.8 ± 1.9%) as compared with control (5.9 ± 1.2%) (Supplementary Figure E5D and E) [9,22]. LY294002 also induced significant morphologic changes, as illustrated in Supplementary Figure E5F. These results indicate that blocking MTOCs completely inhibits the proliferative capacity of human erythroid progenitor cells.

Inhibition of dynein blocks erythroblast enucleation, but not MTOC inhibitors

Time-dependent changes in the enucleation fraction when human D10 erythroblasts were cultured for 72 hours with (Figure 3D showing cell cycles and Fig. 3C, closed circles) or without (Figure 3A showing cell cycles and Fig. 3C, *open circles*) various concentrations of the dynein inhibitor EHNA are provided. Mature untreated erythroblasts differentiated and began the enucleation process (Fig. 3B). EHNA dose-dependently inhibited the increase in the enucleation fraction, and the nucleus remained in the center of cells (Fig. 3E). The absence of a nonspecific effect of EHNA (400 μmol/L) on enucleation was confirmed by the expression of dynein and α-tubulin (Supplementary Figure E6), as well as CD71 and GPA (Supplementary Figure E7). There were no significant differences in the gene expression of GATA1 and GLUT1 after culture of cells for 48 hours with or without EHNA (Supplementary Figure E8). As reported previously, monastrol did not block human erythroblast enucleation (Supplementary Figure E9A–C) [5]. Figure 4 illustrates that none of the MTOC inhibitors tested in this study blocked enucleation.

Morphologic analysis of cells cultured with or without inhibitors

We next assessed the effect of MTOC and motor protein inhibitors on the positioning of the nucleus during terminal differentiation of human D10 erythroblasts (Table 1). The cells were classified as described under Methods and in Supplementary Figure E1. Among these cells, the centered

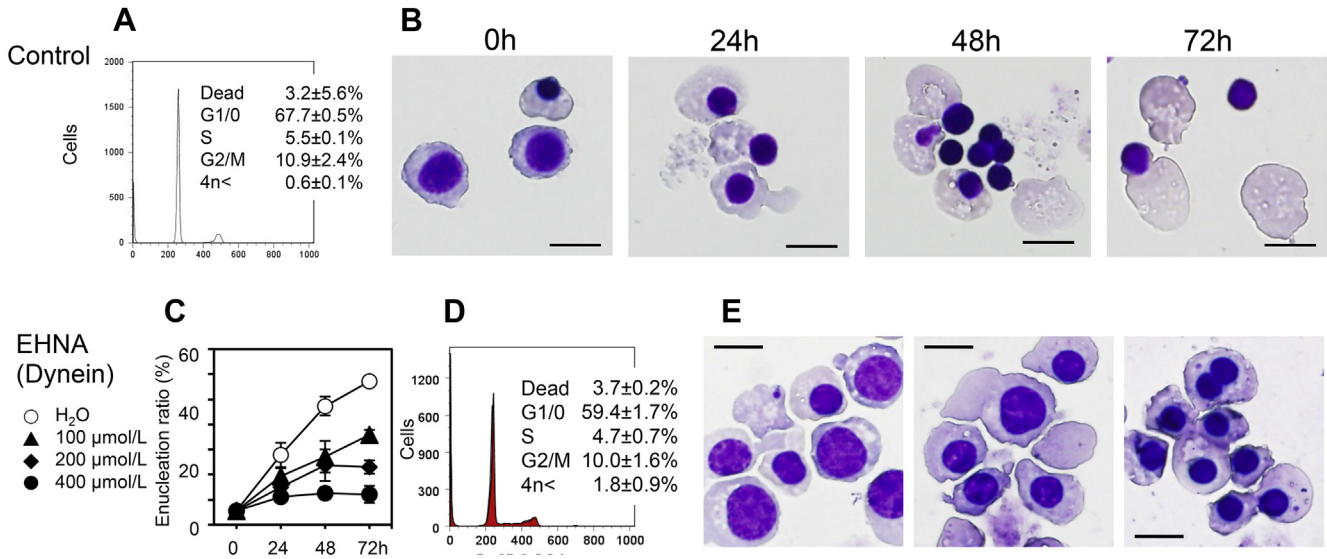

Figure 3. Inhibitors of dynein enucleation of erythroblasts. Human D7 CFU-Es were cultured with EPO for an additional 3 days (until D10). By then they had differentiated to mature erythroblasts at a stage prior to enucleation. Culture was then continued in the presence of EPO with or without inhibitor of dynein (EHNA). (**A**) Cell cycle analysis of D10 cells without inhibitors. (**B**) May–Grünwald–Giemsa staining of D10 cells after culture for 0, 24, 48, or 72 hours without inhibitors. (**C**) Effects of the indicated concentrations of inhibitor or vehicle on enucleation of D10–D13 erythroblasts. Results are presented as means ± SD of three independent experiments. (**D**) Cell cycle analysis of D10 cells after culture for 24 hours with (*red areas*) or without (*black lines*) 400 μmol/L EHNA. A representative result from three independent experiments is presented as the mean ± SD. (**E**) May–Grünwald–Giemsa staining of D11–D13 cells after culture for 24, 48, or 72 hours with or without 400 μmol/L EHNA. A representative result from three independent experiments is shown. Bar = 10 μm.

and polarized cell fractions were 73.0 ± 2.7% (range, 68.5% to 76.1%) and 16.7 ± 1.6% (range, 14.6% to 19.3%), respectively. After incubation of the cells for an additional 24 hours with no inhibitors, the centered and polarized fractions had changed to 46.9 ± 4.4% (range, 43.9%–53.2%) and 21.5 ± 3.1% (range, 15.7%–24.3%), respectively. Over the same 24 h, the reticulocyte fraction increased from 7.7 ± 1.4% (range, 5.3%–9.0%) to 29.6 ± 3.7% (range, 28.0%–30.5%).

Inhibiting dynein using EHNA significantly inhibited the decline in the centered cell fraction and the increase in the reticulocyte fraction that were seen in untreated control cells over the 24-h period from D10 to D11 (Table 1 and Supplementary Figure E10). By contrast, inhibition of kinesin Eg5 using monastrol had no effect on nuclear positioning, nor did inhibition of PI3K. Treatment with the aforementioned inhibitors of Plk1, aurora A, or aurora B led to reductions in the centered cell fraction (Table 1 and Supplementary Figure E10).

Expression of γ-tubulin, motor proteins, and MTOC regulators in human erythroblasts

Because the dynein inhibitor EHNA increased the centered cell fraction in day 10–11 cells and blocked erythroblast enucleation, we investigated the expression of MTOC-related proteins during terminal differentiation of human erythroblasts. γ-Tubulin was immunochemically detected in the cytoplasm in erythroblasts from D7 (CFU-E) to D13 (late-stage erythroblasts and reticulocytes) (Fig. 5), and the expression of γ-tubulin did not to change during that period. Western blotting revealed that dynein was expressed during terminal erythroblast differentiation (Fig. 5). Little or no Eg5, Plk1, aurora A or aurora B was expressed in D13 (Fig. 5). These results suggest dynein is a key regulator of nuclear positioning and enucleation in terminally differentiated erythroblasts.

Distribution of dynein and γ-tubulin in erythroblasts during terminal differentiation

In D7 CFU-Es, γ-tubulin was immunochemically detected around the periphery of the nucleus and in the cleavage furrow, and α-tubulin (microtubules) was localized around the γ-tubulin (Fig. 6A). In D11 cells, the nucleus was displaced to one side of the cell, and γ-tubulin was located in the center of cell (Supplementary Figure E11). Although dynein was broadly distributed in the cytoplasm and did not co-localize with α-tubulin in D8 cells, in D11 cells, it was distributed in aggregates on the periphery of the nucleus and co-localized with α-tubulin at or near the MTOCs (Fig. 6B and Supplementary Figure E12 containing high-magnification images). Treating the D10 cells with 400 μmol/L EHNA blocked dynein aggregation such that it remained diffuse in the cytoplasm (Fig. 6B). In contrast to dynein, Eg5 co-localized with α-tubulin at the cleavage furrow in mitotic CFU-Es (Supplementary Figure E13A). In D7 and D8 CFU-Es, Plk1 and aurora B also co-localized with α-tubulin at the cleavage furrow (Supplementary Figure E13B and D), and aurora A localized around the spindles in D7 cells (Supplementary Figure E13C). But little if any Eg5, Plk1, aurora A, or

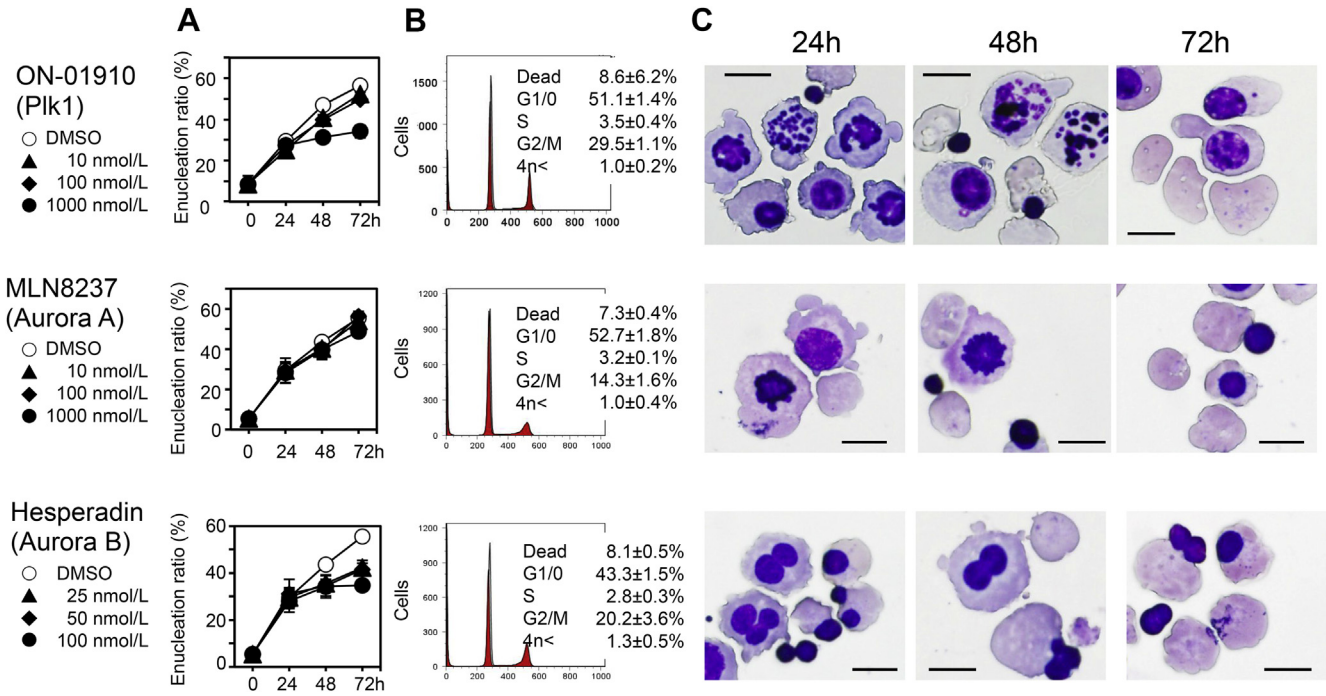

Figure 4. Inhibitors of MOTCs do not block erythroblast enucleation. D10 cells were cultured for 3 days in the presence of EPO with or without the inhibitors Plk1 (ON-01910), aurora A (MLN8237), and aurora B (hesperadin). (**A**) Effects of the indicated concentrations of inhibitors or vehicle on enucleation of D11–D13 erythroblasts. Results are presented as the means ± SD of three independent experiments. (**B**) Cell cycle analysis of D11 cells after culture for 24 hours with (*red areas*) or without (*black lines*) 1,000 nmol/L ON-01910, 1,000 nmol/L MLN8237, or 100 nmol/L hesperadin. A representative result from three independent experiments is presented as the mean ± SD. (**C**) May–Grünwald–Giemsa staining of D11–D13 cells after culture for 24, 48, or 72 hours with or without 1,000 nmol/L ON-01910, 1,000 nmol/L MLN8237, or 100 nmol/L hesperadin. A representative result from three independent experiments is shown. Bar = 10 μm.

aurora B was detected in D11 cells (Supplementary Figure E13A–D). Taken together, these results suggest that accumulation of dynein around the MTOCs is necessary for polarization and subsequent enucleation of erythroblasts.

Discussion

In the present study, we found that among the motor proteins and MTOC regulatory proteins tested, only dynein was necessary for cell division and nuclear polarization during terminal differentiation and enucleation. Kinesin Eg5 and the MTOC regulators Plk1, aurora A, and aurora B were absent or dispensable. Our findings thus indicate that enucleation is a process apparently independent of MTOC-related proteins, but dependent on dynein.

During differentiation of CFU-Es into mature erythroblasts lacking the ability to divide, the cells repeatedly undergo mitosis and cytokinesis. Furthermore, CFU-Es will not differentiate into erythroblasts if mitosis or cytokinesis is inhibited. On the other hand, enucleation of human erythroblasts does not require mitosis. Because the relation between inhibition of cell division or maturation and blocking of enucleation is conflated in some reports, we suggest it is important for studies to clearly distinguish erythroblast enucleation from mitosis and cytokinesis. Our present study satisfies that condition, as we compared CFU-E mitosis and cytokinesis with nonproliferating mature erythroblasts.

Thom et al. reported that Trim58 functions as an E3 ubiquitin ligase that facilitates protein degradation and is expressed during terminal differentiation of human and mouse erythroblasts [23]. Moreover, they suggest that Trim58-mediated complete dynein degradation may be responsible for nuclear movement during enucleation. We also compared the expression of Trim58 and dynein immunochemically using antibodies targeting dynein intermediate chain 1 or dynein light intermediate chain 2. Like Thom et al, we found that Trim58 levels increased during the period from D7 to D13. But in contrast to those investigators, we found that low levels of dynein persisted within human erythroblasts throughout their terminal differentiation (Supplementary Figure E14). Apparently, complete degradation of dynein is not essential for cell polarization prior to enucleation of human erythroblasts. Notably, Thom et al. used mouse fetal liver erythroblasts, whereas we used erythroblasts derived from human $CD34^{+}$ cells purified from peripheral blood [23]. The discrepancy between our results and those of Thom et al. may reflect this species difference.

Table 1. Morphologic analysis of cells cultured with or without inhibitors*

Inhibitor	Centered	Polarized	Other	Reticulocytes
Control				
0 h	76.1 ± 3.3	16.0 ± 2.9	1.2 ± 0.2	6.7 ± 0.7
−24 h	48.1 ± 6.3	22.9 ± 3.7	1.0 ± 0.6	28.0 ± 5.5
EHNA 400 μmol/L	67.4 ± 1.9†	21.0 ± 2.1	0.4 ± 0.5	11.1 ± 0.7‡
Control				
0 h	75.3 ± 1.7	16.9 ± 2.6	2.3 ± 1.0	5.5 ± 1.8
−24 h	43.9 ± 5.2	23.4 ± 2.1	2.3 ± 1.9	30.5 ± 8.0
Monastrol 100 μmol/L	47.1 ± 3.7	21.1 ± 2.1	5.3 ± 3.1	26.6 ± 5.0
Control				
0 h	68.5 ± 2.9	19.3 ± 3.5	13.6 ± 1.6	8.7 ± 3.6
−24 h	46.2 ± 1.9	23.2 ± 3.7	2.4 ± 1.7	28.1 ± 1.0
ON-01910 1,000 nmol/L	33.1 ± 5.4§	15.3 ± 2.7§	19.9 ± 1.7†	31.7 ± 5.5
Control				
0 h	73.3 ± 2.3	18.2 ± 1.7	3.1 ± 0.5	5.3 ± 1.5
−24 h	47.4 ± 2.7	21.5 ± 4.3	2.6 ± 1.5	28.5 ± 1.3
MLN8237 1,000 nmol/L	52.6 ± 5.3	15.9 ± 0.7	3.6 ± 0.8	28.0 ± 4.1
Hesperadin 100 nmol/L	33.6 ± 2.5‡	20.7 ± 2.9	17.7 ± 2.0†	28.1 ± 3.6
Control				
0 h	73.0 ± 2.2	18.4 ± 2.7	1.4 ± 1.0	7.3 ± 0.7
−24 h	46.0 ± 1.2	24.3 ± 3.8	1.1 ± 0.9	28.7 ± 3.9
LY294002 100 μmol/L	48.4 ± 6.3	26.0 ± 3.1	0.6 ± 0.2	25.1 ± 3.7

EHNA = erythro-9-[3-(2-hydroxynonyl)]adenine.
*Centered refers to cells in which the nucleus was localized at the center of the cell. Polarized refers to spherical cells, which contained a condensed nucleus located to one side, near the plasma membrane. Reticulocytes refer to enucleated c. Other cell types, such as multinucleate cells and cells with condensed apoptotic nuclei, were classified as "other." Images of cells classified as described are shown in Supplementary Figure E1 (online only, available at www.exphem.org). The fractions of each cell type were calculated as described in the text. Results are presented as the mean ± SD of three independent experiments.
†Significantly increased, $p < 0.01$.
‡Significantly decreased, $p < 0.01$.
§Significantly decreased, $p < 0.05$.

Consistent with that idea, the time for terminal differentiation of erythroblasts from CFU-Es was 7 days in humans, but only 2 days in mice. Although knockdown of dynein or Trim58 in our system should be considered to explain this discrepancy, we have not yet succeeded in transfecting the siRNA and/or its expression vectors. Further experiments are needed to clarify this discrepancy.

Dynein mediates unidirectional nuclear movement toward MTOCs, whereas kinesin Eg5 walks toward the plus end of microtubules [14,16,24,25]. We observed that moving the nucleus requires dynein, but not Eg5, and that dynein accumulates at or near MTOCs in D11 cells (Fig. 6B). It is not yet known precisely what dynein carries from the plasma membrane to MTOCs in human erythroblasts. Keerthivasan et al.

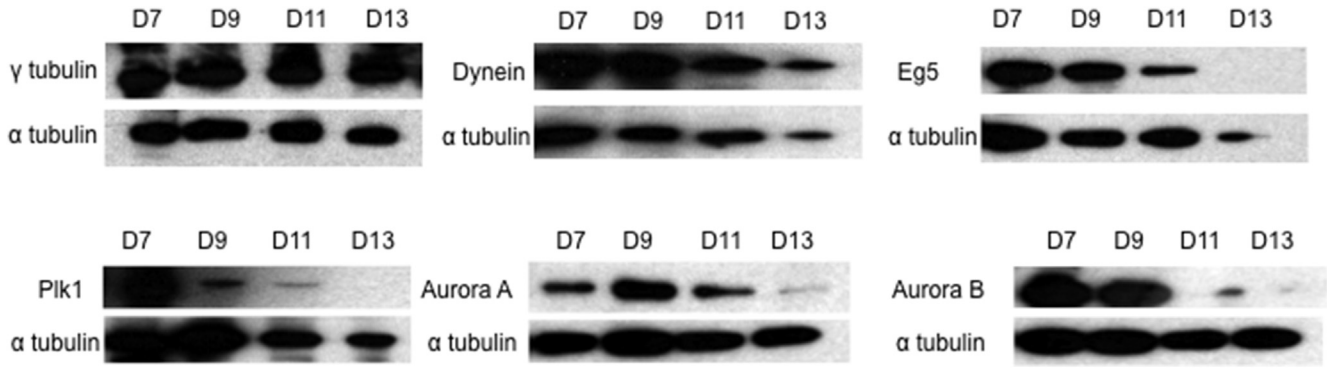

Figure 5. Expression of dynein, Eg5, and MTOC regulators during human erythropoiesis. Western blot analyses of human CFU-Es (D7), erythroblasts (D9 and D11), and enucleated cells (D13). Human CFU-Es were generated from purified $CD34^+$ cells and cultured for the indicated periods in the presence of EPO. Protein collected from 1×10^5 D7–D13 cells was applied to each lane. Expression of γ-tubulin, dynein, Eg5, aurora A, aurora B, and Plk1 was analyzed. The relative expression levels of the proteins were normalized to the level of α-tubulin expression. Anti-dynein light intermediate chain 1 was employed for the Western blot.

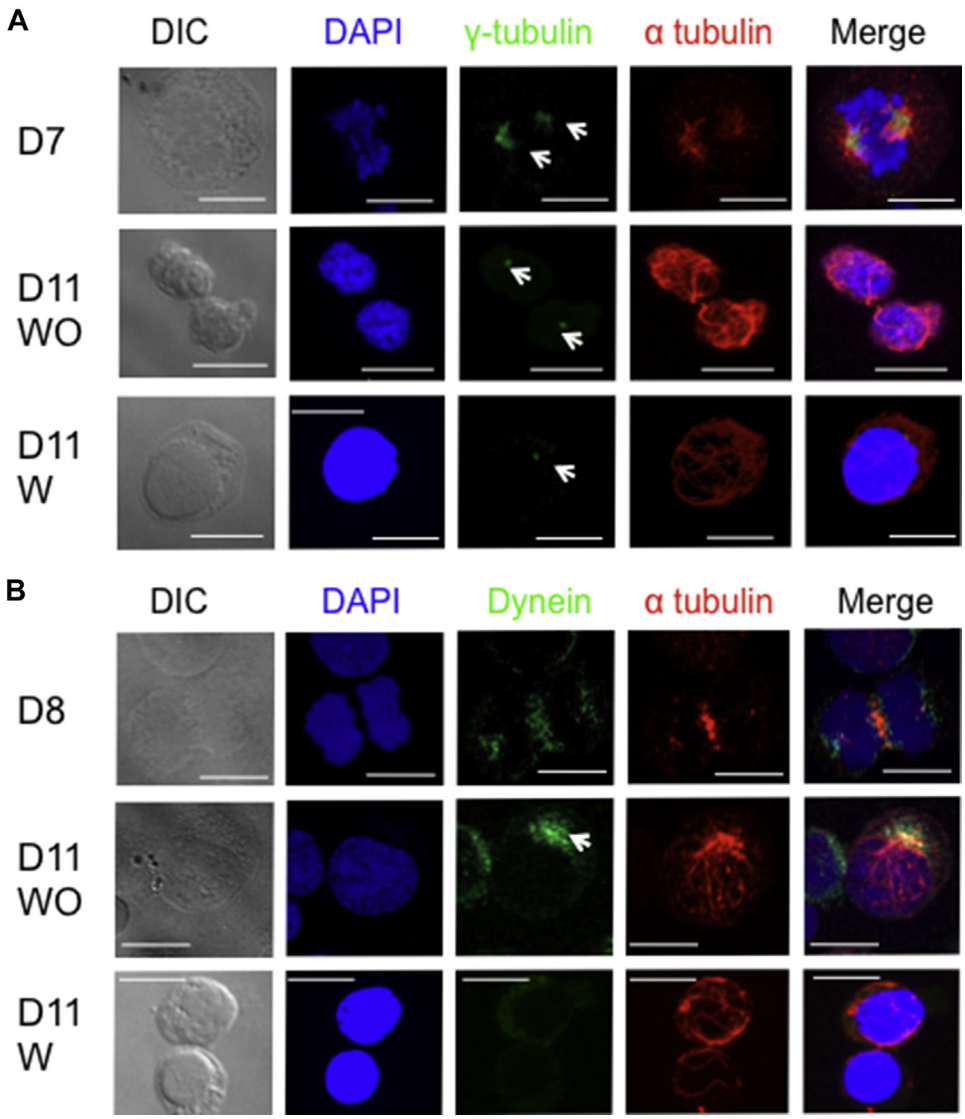

Figure 6. Distribution of tubulin and dynein in D11 cells with or without EHNA treatment. Confocal micrographs of CFU-Es (D7 or D8) and erythroblasts (D11) stained with DAPI (*blue*) or antibodies against γ-tubulin (**A**) or dynein (*green*, anti-dynein light intermediate chain 1 antibody was employed, (**B**) and α-tubulin (*red*). Overlapping staining in the merged images is shown in *yellow*. Differential interference contrast microscopic image (DIC) is shown. W and WO respectively denote D10 cells treated for 24 hours with and without 400 μmol/L EHNA. Bar = 10 μm.

reported that in mouse fetal liver erythroblasts, vesicles accumulate at the site of nuclear extrusion and form a vacuole essential for enucleation, and that enucleation is blocked by inhibitors for vesicle trafficking [26]. Those results illustrate that the function of dynein in the enucleation of human erythroblasts is the trafficking of vesicles. It has also been suggested that dynein may be anchored to the nucleus through some unidentified molecule(s) within erythroblasts. Then through a mechanism whereby dynein binds to γ-tubulin and is pulled toward the plus end of the microtubule, the nucleus anchored to dynein is pulled along with it [25,27,28]. Within that scenario, EHNA could affect the dynein-containing complex such that enucleation is inhibited.

Alternatively, it is known that dynein anchored to the cytoplasmic membrane through the nuclear mitotic apparatus (NuMA) pulls on microtubules bound to γ-tubulin in MTOCs [27]. It is also known that the plus ends of microtubules are anchored to NuMA and that NuMA is a key component, along with LGN (Leu–Gly–Asn repeat-enriched protein) and $Gi\alpha^{GDP}$ protein, of the ternary complexes that form at the plus end of microtubles [29,30]. However, nuclear localization of NuMA in mouse erythroblasts has been reported [31]. This suggests human erythroblasts also may not contain dynein–NuMA complexes anchored to the cytoplasmic membrane. The precise mechanism of nuclear localization dependent on the dynein will be clarified in future investigations.

We are confident that blockade of enucleation by the dynein inhibitor EHNA is a specific effect. We

observed an inhibitory effect of 50 μmol/L EHNA (data not shown) on CFU-E proliferation and of 400 μmol/L on EHNA-blocked enucleation (Fig. 3). In previous reports, the IC_{50} of EHNA for dynein ATPase was 0.23 mmol/L, and this inhibitor is normally used at concentrations ranging from 0.5 to 2 mmol/L [20,28]. Furthermore, no inhibitory effects of EHNA (at 0.23 mmol/L) on actomyosin or other ATPases or glycolytic enzymes have been reported [20]. As we presented in this study, no multinucleate cells, which are produced by actin inhibition with cytochalasin D, appeared on EHNA treatment. The results indicated that EHNA specifically inhibits dynein without side effects.

Wang et al. reported that enucleation requires establishment of cell polarization that is regulated by the microtubule-dependent local activation of PI3K, and that its products, phosphatidylinositol 3,4-diphosphate and phosphatidylinositol 3,4,5-triphosphate, are highly localized on the cytoplasmic side of the plasma membrane [9]. These inositol phosphates may be useful in determining the origin of the enucleation site, as PI3K activation could be identified as the initial signal for erythroblast enucleation. Wang et al. proposed that enucleation is regulated by microtubules and PI3K signaling in a manner mechanistically similar to that of directed cell locomotion [9]. In their study, α-tubulin was concentrated at the opposite side of the nucleus and few microtubule fibers were found in the periphery of the nucleus. Future experiments are needed to clarify the relationship between enucleation and cell locomotion.

In conclusion, our findings indicate dynein is a key mediator of cell division and nuclear polarization during terminal differentiation and enucleation of human erythroblasts. By contrast, enucleation is independent of most MTOC-related proteins.

Acknowledgments

This work was supported in part by JSPS KAKENHI Grants 23591412, 25860777, 26461439, 15K19540, and 15K09448, and research grants from the SENSHIN Medical Research Foundation and the Idiopathic Disorders of Hematopoietic Organs Research Committee of the Ministry of Health, Labour and Welfare of Japan.

The authors are grateful to Hiromi Kataho and Etsuko Kobayashi from the Department of Hematology, Nephrology, and Rheumatology, Akita University Graduate School of Medicine, for their valuable technical assistance.

Conflict of interest disclosure

No financial interest/relationships relating to the topic of this article have been declared.

References

1. Hebiguchi M, Hirokawa M, Guo YM, et al. Dynamics of human erythroblast enucleation. Int J Hematol. 2008;88:498–507.
2. Oda A, Sawada K, Druker BJ, et al. Erythropoietin induces tyrosine phosphorylation of Jak2, STAT5A, and STAT5B in primary cultured human erythroid precursors. Blood. 1998;92:443–451.
3. Sawada K, Krantz SB, Kans JS, et al. Purification of human erythroid colony-forming units and demonstration of specific binding of erythropoietin. J Clin Invest. 1987;80:357–366.
4. Sawada K, Krantz SB, Dai CH, et al. Transitional change of colony stimulating factor requirements for erythroid progenitors. J Cell Physiol. 1991;149:1–8.
5. Ubukawa K, Guo YM, Takahashi M, et al. Enucleation of human erythroblasts involves non-muscle myosin IIB. Blood. 2012;119:1036–1044.
6. Chasis JA, Mohandas N. Erythroblastic islands: Niches for erythropoiesis. Blood. 2008;112:470–478.
7. Glotzer M. The molecular requirements for cytokinesis. Science. 2005;307:1735–1739.
8. Barr FA, Gruneberg U. Cytokinesis: placing and making the final cut. Cell. 2007;131:847–860.
9. Wang J, Ramirez T, Ji P, et al. Mammalian erythroblast enucleation requires PI3K-dependent cell polarization. J Cell Sci. 2012;125(Pt 2):340–349.
10. Brinkley BR. Microtubule organizing centers. Annu Rev Cell Biol. 1985;1:145–172.
11. Mardin BR, Schiebel E. Breaking the ties that bind: New advances in centrosome biology. J Cell Biol. 2012;197:11–18.
12. Rodionov V, Nadezhdina E, Borisy G. Centrosomal control of microtubule dynamics. Proc Natl Acad Sci U S A. 1999;96:115–120.
13. Tanenbaum ME, Medema RH. Mechanisms of centrosome separation and bipolar spindle assembly. Dev Cell. 2010;19:797–806.
14. Splinter D, Tanenbaum ME, Lindqvist A, et al. Bicaudal D2, dynein, and kinesin-1 associate with nuclear pore complexes and regulate centrosome and nuclear positioning during mitotic entry. PLoS Biol. 2010;8:e1000350.
15. Gomes ER, Jani S, Gundersen GG. Nuclear movement regulated by Cdc42, MRCK, myosin, and actin flow establishes MTOC polarization in migrating cells. Cell. 2005;121:451–463.
16. Laan L, Rothb S, Dogteromb M. End-on microtubule–dynein interactions and pulling- based positioning of microtubule organizing centers. Cell Cycle. 2015;11:3750–3757.
17. Wordeman L. How kinesin motor proteins drive mitotic spindle function: Lessons from molecular assays. Semin Cell Dev Biol. 2010;21:260–268.
18. Hirokawa N, Tanaka Y. Kinesin superfamily proteins (KIFs): Various functions and their relevance for important phenomena in life and diseases. Exp Cell Res. 2015;334:16–25.
19. Vicente JJ, Wordeman L. Mitosis, microtubule dynamics and the evolution of kinesins. Exp Cell Res. 2015;334:61–69.
20. Penningroth SM, Cheung A, Bouchard P, et al. Dynein ATPase is inhibited selectively in vitro by erythro-9-[3-2-(hydroxynonyl)]adenine. Biochem Biophys Res Commun. 1982;104:234–240.
21. Sarli V, Giannis A. Targeting the kinesin spindle protein: basic principles and clinical implications. Clin Cancer Res. 2008;14:7583–7587.
22. Haseyama Y, Ki Sawada, Oda A, et al. Phosphatidylinositol 3-kinase is involved in the protection of primary cultured human erythroid precursor cells from apoptosis. Blood. 1999;94:1568–1577.
23. Thom CS, Traxler EA, Khandros E, et al. Trim58 degrades Dynein and regulates terminal erythropoiesis. Dev Cell. 2014;30:688–700.
24. Van Heesbeen RG, Raaijmakers JA, Tanenbaum ME, Medema RH. Nuclear envelope- associated dynein cooperates with Eg5 to drive prophase centrosome separation. Commun Integr Biol. 2013;6:e23841.

25. Ferenz NP, Paul R, Fagerstrom C, Mogilner A, Wadsworth P. Dynein antagonizes Eg5 by crosslinking and sliding antiparallel microtubules. Curr Biol. 2009;19:1833–1838.
26. Keerthivasan G, Small S, Liu H, et al. Vesicle trafficking plays a novel role in erythroblast enucleation. Blood. 2010;116:3331–3340.
27. Radulescu AE, Cleveland DW. NuMA after 30 years: The matrix revisited. Trends Cell Biol. 2010;20:214–222.
28. Hashimoto-Tane A, Yokosuka T, Sakata-Sogawa K, et al. Dynein-driven transport of T cell receptor microclusters regulates immune synapse formation and T cell activation. Immunity. 2011;34:919–931.
29. Kiyomitsu T. Mechanisms of daughter cell-size control during cell division. Trends Cell Biol. 2015;25:286–295.
30. Mapelli M, Gonzalez C. On the inscrutable role of Inscuteable: structural basis and functional implications for the competitive binding of NuMA and Inscuteable to LGN. Open Biol. 2012;2:120102.
31. Krauss SW, Lo AJ, Short SA, et al. Nuclear substructure reorganization during late-stage erythropoiesis is selective and does not involve caspase cleavage of major nuclear substructural proteins. Blood. 2005;106:2200–2205.

Supplementary methods

Reagents and antibodies

Bovine serum albumin (BSA), Iscove's modified Dulbecco's medium (IMDM), and propidium iodide (PI) were purchased from Sigma-Aldrich (St. Louis, MO). Fetal calf serum (FCS) was from Flow Laboratories (McLean, VA) and Hyclone Laboratories (Logan, UT). Penicillin and streptomycin were from Flow Laboratories. Insulin (porcine sodium; activity, 28.9 U/mg) was from Wako Pure Chemical Industries (Osaka, Japan). Interleukin-3 (IL-3) and stem cell factor (SCF) were kind gifts from Kirin Brewery (Tokyo, Japan). Erythropoietin (EPO) and granulocyte colony-stimulating factor (G-CSF) were gifts from Chugai Pharmaceutical (Tokyo, Japan). Vitamin B_{12} was from Eisai (Tokyo, Japan), and folic acid was from Takeda Pharmaceutical (Osaka, Japan). Triton X-100 was from Wako Pure Chemical Industries (Osaka, Japan). MACS MicroBeads for Indirect Magnetic Labeling were from Miltenyi Biotec (Bergisch-Gladbach, Germany). Alexa Fluor 488- and Alexa Fluor 546-conjugated goat anti-rabbit and anti-mouse IgGs were from Molecular Probes (Eugene, OR). Fc-blocking antibody (anti-CD16/32, Clone: 93) was from eBioscience (San Diego, CA). Normal mouse and goat sera and rabbit immunoglobulins were from Cell Signaling Technology (Beverly, MA). Mouse monoclonal anti-α-tubulin antibody was from Neo Markers (Fremont, CA). Rabbit polyclonal anti-γ-tubulin antibody was from Abcam (Cambridge, MA). Rabbit monoclonal anti-aurora A antibody was from Cell Signaling Technology (Beverly, MA). Rabbit polyclonal anti-aurora B antibody was from Abcam (Beverly, MA). Rabbit monoclonal anti-cytoplasmic dynein 1, monoclonal anti-dynein light intermediate chain 1, polyclonal anti-Eg5 and polyclonal anti-Trim58 were from Abcam (Cambridge, MA). Goat anti-mouse IgG–HRP was from Santa Cruz Biotechnology (Santa Cruz, CA). DAPI (4′,6-diamidino-2-phenylindole, dihydrochloride) was from Life Technologies Invitrogen. Fluorescein isothiocyanate (FITC)-labeled anti-glycophorin A (GPA-FITC) were purchased from Dako Japan (Tokyo, Japan), and phosphoerythrin (PE)-labeled anti-CD71 (CD71-PE) was purchased from BD Biosciences (Franklin Lakes, NJ). ECL Plus Western Blotting Detection Reagents were from GE Healthcare UK (Buckinghamshire, UK). Novex Sharp Protein Standard and NuPAGE Novex Bis-Tris Mini Gels were from Life Technologies Invitrogen.

Inhibitors

Erythro-9-[3-(2-hydroxynonyl)]adenine (EHNA), a dynein inhibitor, was from Millipore (Billerica, MA) [20]. Monastrol, an inhibitor of kinesin Eg5, was from Merck (Whitehouse Station, NJ) [21]. ON-01910, an inhibitor of polo-like kinase (Plk) 1, and MLN8237, an inhibitor of aurora A, were from Selleck Chemicals (Houston, TX) [32–35]. Hesperadin, an inhibitor of aurora B, and LY294002, an inhibitor of PI3K, were from Cell Signaling Technology (Beverly, MA) [9,26,36].

Evaluation of enucleation

To evaluate enucleation, cells were spun onto slides using a Cytospin 3 (Shandon Lipshaw, Pittsburgh, PA) and stained with May–Grünwald–Giemsa. Enucleation was defined as the expulsion of the nucleus to the outside of the reticulocyte. Reticulocytes touching expelled nuclei or with a thin connecting strand between the reticulocyte and nucleus were considered the earliest enucleated cells. The enucleation fraction among the cytospin cells was similar to that among cells prepared without mechanical force. The enucleation fraction was calculated using the formula (erythrocytes/[erythrocytes + erythroblasts]) × 100 (%) with 300 cells, including erythrocytes and erythroblasts, from each slide [5]. Triplicate cultures were used at each time point. The yield and viability were determined based on dye exclusion using 0.2% trypan blue dye [5].

Cell cycle distribution

Cells were harvested, washed with cold 10 mmol/L Na_2HPO_4/NaH_2PO_4, pH 7.4, containing 0.15 mol/L NaCl (phosphate-buffered saline [PBS]), fixed in 70% ethanol, and then stored at −20°C until analysis. The fixed cells were centrifuged at 1,200 rpm and washed with cold PBS twice, after which RNase A was added to a final concentration of 0.5 mg/mL, and the cells were incubated for 10 min at 37°C. Thereafter, 25 μg/mL PI was added, and the cells were incubated for 30 min at room temperature in the dark. The cells were then analyzed using a FACS Calibur instrument (BD Biosciences, San Jose, CA) equipped with CellQuest 3.3 software as reported previously [5,22,37]. FlowJo Version 7.2.5 (TOMY Digital Biology, Tokyo, Japan) was used to determine the cell fractions (%) in the different cell cycle phases.

Confocal microscopy

Conventional immunocytochemical staining was performed as described previously [38]. For three-image immunocytochemical staining, the cells were immobilized on poly-L-lysine-coated slide glass. Fluorescence staining was imaged using two confocal laser scanning microscopes (LSM510 and LSM710, Carl Zeiss Microscope Systems, Germany) equipped with 100× objective lenses and 10× camera lenses (Carl Zeiss Microscope Systems) at zoom 3, as reported elsewhere [5]. Fluorochromes were excited using an argon laser at 488 nm for Alexa 488. Detector slits were configured to minimize cross-talk between channels and processed using ZEN2012 Version 3.2 (Zeiss) and Photoshop (Adobe Systems).

Morphologic and immunochemical analysis of cells cultured with and without inhibitors

The cells were classified based on the whether the nucleus was localized at the center of the cells (centered); the cells

were spherical containing a condensed nucleus located to one side, close to the plasma membrane (polarized); or the cells were enucleated (reticulocytes). Other cell types, such as multinucleate cells and cells with condensed apoptotic nuclei, were classified as "other." Images of cells classified as described are provided in Supplementary Figure E1 (online only, available at www.exphem.org). The fractions of each cell type were calculated as described under Evaluation of Enucleation. Results are presented as the mean ± SD of three independent experiments.

Immunochemical distributions of γ-tubulin and dynein were determined using confocal microscopy as described above. D10 cells were cultured in the presence or absence of 400 μmol/L EHNA.

Western blot analysis

$CD34^+$ cells were incubated in erythroid medium for the indicated times. Western blot analysis was carried out as described previously [5].

Flow cytometry

Cells collected from culture were first washed twice with IMDM containing 0.3% BSA. They were then incubated with FITC-conjugated anti-glycophorin A (GPA) and PE-conjugated CD71, washed twice with staining medium (10 mmol/L PBS, pH 7.4, 0.5% BSA, and 2 mmol/L EDTA) and analyzed [37].

Real-time RT-PCR

Total RNA was extracted from 2×10^4 cells per sample using TRizol reagent (Invitrogen). The extracted RNA was then reverse-transcribed using a SuperScript III First-Strand Synthesis System for reverse transcription polymerase chain reaction (RT-PCR, Invitrogen) in a 20-μL reaction volume. The resultant cDNA was subjected to real-time RT-PCR using LightCycler 480 SYBR Green I Master (Roche Applied Science). Relative gene expression levels were normalized to 28 S. The primers used to assess GATA1 and GLUT1 expression were purchased from Sigma Japan (Tokyo, Japan). Their sequences are as follows:

GATA1:
5′-TCTGGACAACCCAAGTCTCTG-3′ (forward)
5′-GGCTTGAACCTTCAAAGC-3′ (reverse) (GenBank ID: BC009797)

GLUT1:
5′-ATACTCATGACCATCGCGCTAG-3′ (forward)
5′-AAAGAAGGCCACAAAGCCAAAG-3′ (reverse) (GenBank ID: BC118590.1) [39,40].

Statistical analysis

Statistical analysis was performed using Student's *t* test for parametric data and the Mann–Whitney *U* test for nonparametric data. Two-tailed *p* values <0.05 were considered to indicate significance.

Supplementary references

32. Schöffski P. Polo-like kinase (PLK) inhibitors in preclinical and early clinical development in oncology. Oncologist. 2009;14:559–570.
33. Bruinsma W, Raaijmakers JA, Medema RH. Switching polo-like kinase-1 on and off in time and space. Trends Biochem Sci. 2012;37:534–542.
34. Görgün G, Calabrese E, Hideshima T, et al. A novel aurora-A kinase inhibitor MLN8237 induces cytotoxicity and cell-cycle arrest in multiple myeloma. Blood. 2010;115:5202–5213.
35. Hochegger H, Hégarat N, Pereira-Leal JB. Aurora at the pole and equator: Overlapping functions of aurora kinases in the mitotic spindle. Open Biol. 2013;3:120185.
36. Carmena M, Ruchaud S, Earnshaw WC. Making the auroras glow: Regulation of aurora A and B kinase function by interacting proteins. Curr Opin Cell Biol. 2009;21:796–805.
37. Guo YM, Ishii K, Hirokawa M, et al. CpG-ODN 2006 and human parvovirus B19 genome consensus sequences selectively inhibit growth and development of erythroid progenitor cells. Blood. 2010;115:4569–4579.
38. Saito K, Hirokawa M, Inaba K, et al. Phagocytosis of codeveloping megakaryocytic progenitors by dendritic cells in culture with thrombopoietin and tumor necrosis factor-alpha and its possible role in hemophagocytic syndrome. Blood. 2006;107:1366–1374.
39. Moriguchi T, Yu L, Takai J, et al. The human GATA1 gene retains a 5' insulator that maintains chromosomal architecture and GATA1 expression levels in splenic erythroblasts. Mol Cell Biol. 2015;35:1825–1837.
40. Pérez de Heredi F, Wood IS, Trayhurn P. Hypoxia stimulates lactate release and modulates monocarboxylate transporter (MCT1, MCT2, and MCT4) expression in human adipocytes. Eur J Physiol. 2010;459:509–518.

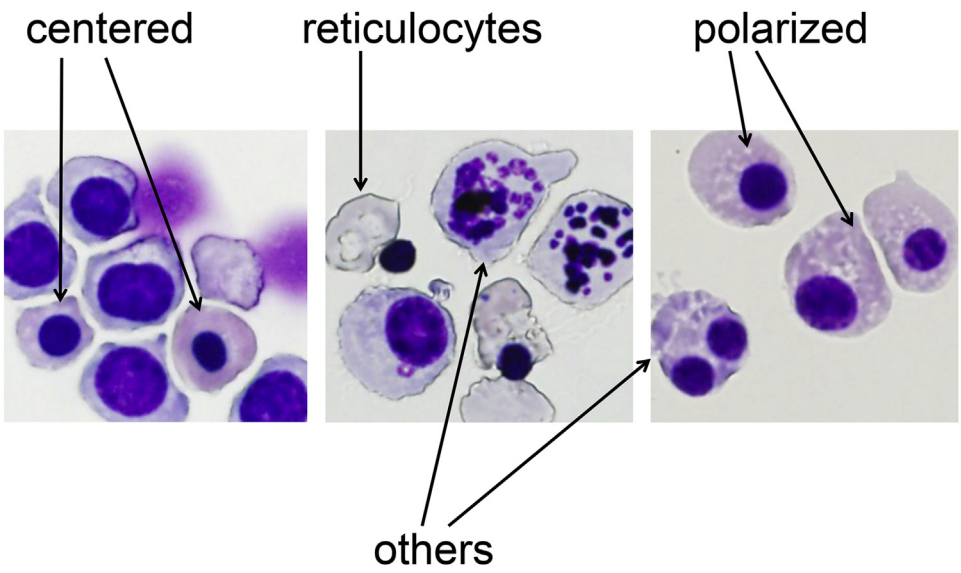

Supplementary Figure E1. Shown are typical cells classified as *centered* (nucleus localized at the center of the cells), *reticulocyte* (enucleated reticulocyte), *polarized* (spherical cells containing a condensed nucleus located to one side, close to the plasma membrane), and other (apoptotic or multinucleate). Cells are stained with May–Grünwald–Giemsa reagent.

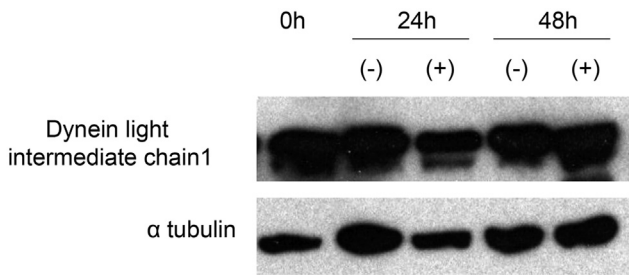

Supplementary Figure E2. Dynein expression in CFU-Es (D7) incubated with and without EHNA (400 μmol/L) was analyzed by Western blotting with an antibody against dynein light intermediated chain 1. α-Tubulin served as an internal control. Note that dynein was expressed in the presence of EHNA, indicating the inhibitor did not affect dynein protein expression in CFU-Es.

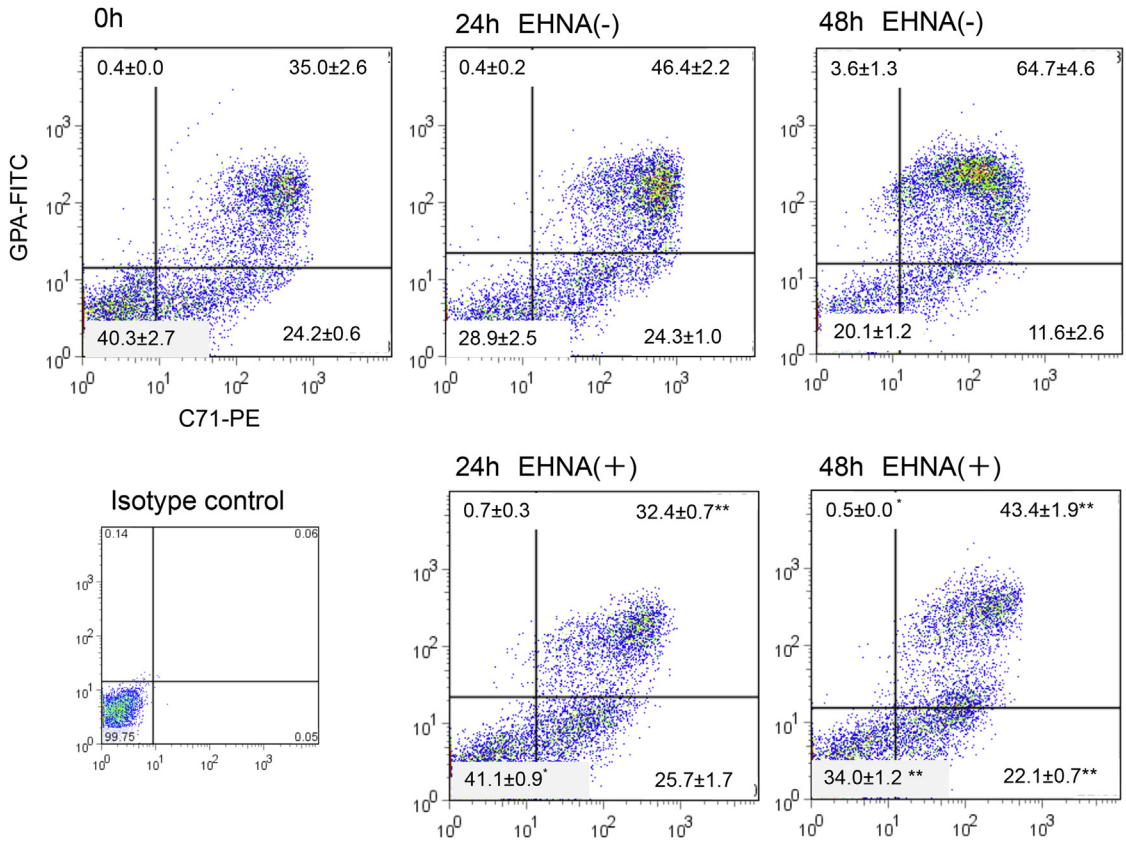

Supplementary Figure E3. To confirm the absence of a nonspecific effect of EHNA on protein expression, the CFU-E populations expressing CD71 and glycophorin A (GPA) in the presence and absence of EHNA (400 μmol/L) were analyzed using flow cytometry. The results indicate that EHNA blocked proliferation of CFU-Es by inhibiting dynein.

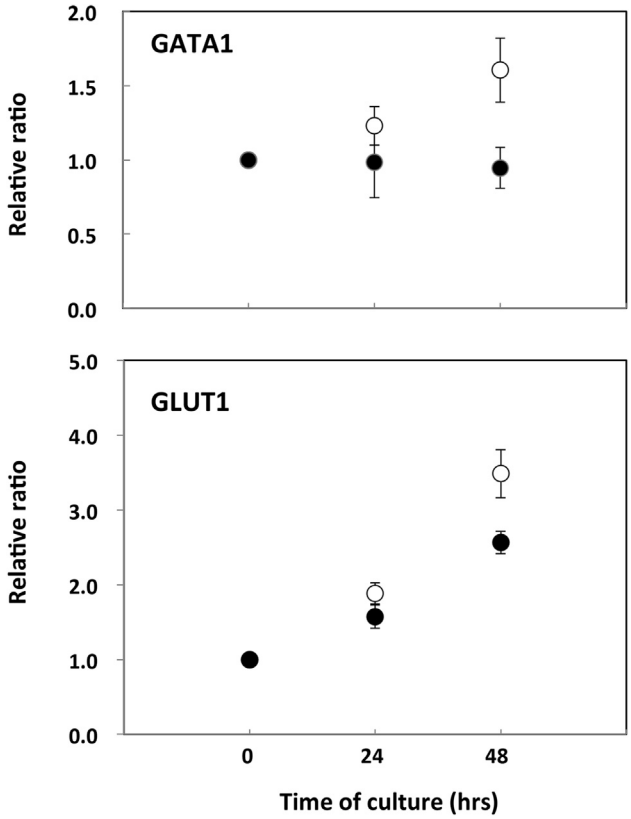

Supplementary Figure E4. Real-time RT-PCR of GATA1 and GLUT1 in CFU-Es treated with (●) or without (○) EHNA. Three independent experiments were performed, and the data are presented as the average and SE. There were no significant differences between CFU-Es incubated for 24 hours with or without EHNA.

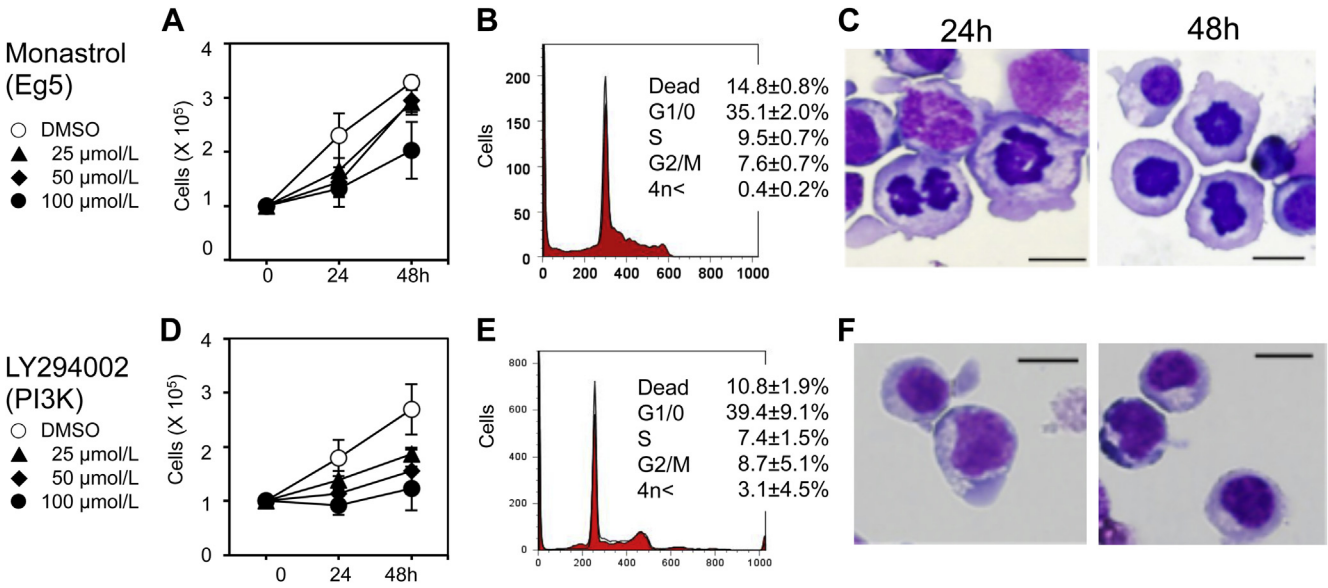

Supplementary Figure E5. Human D7 CFU-Es generated from purified $CD34^+$ cells were cultured for the indicated periods in the presence of EPO with or without inhibitors of Eg5 (monastrol, **A**–**C**) or PI3K (LY294002, **D**–**F**). (**A**, **D**) Effects of the indicated concentrations of inhibitors or vehicle on CFU-E proliferation. Results are presented as the means ± SD of three independent experiments. (**B**, **E**) Cell cycle analysis of D8 cells after culture for 24 hours with (*red areas*) or without (*solid lines*). A representative result from three independent experiments is presented as the mean ± SD. (**C**, **F**) May–Grünwald–Giemsa staining of D8–D9 cells after culture for 24 or 48 hours with or without 100 μmol/L monastrol (**C**) and 100 μmol/L LY294002 (**F**). A representative result from three independent experiments is shown. Bar = 10 μm. Note that after 7 days of culture (D7) in the presence of monastrol, however, cells of various sizes were observed, some with condensed nuclei (deeply stained).

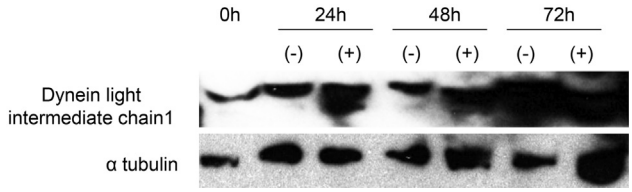

Supplementary Figure E6. Dynein expression in D10 cells incubated with and without EHNA (400 μmol/L) was analyzed by Western blotting with an antibody against dynein light intermediated chain 1. α-Tubulin served as an internal control. Note that dynein was expressed in the presence of EHNA, indicating the inhibitor did not affect dynein protein expression in D10 cells.

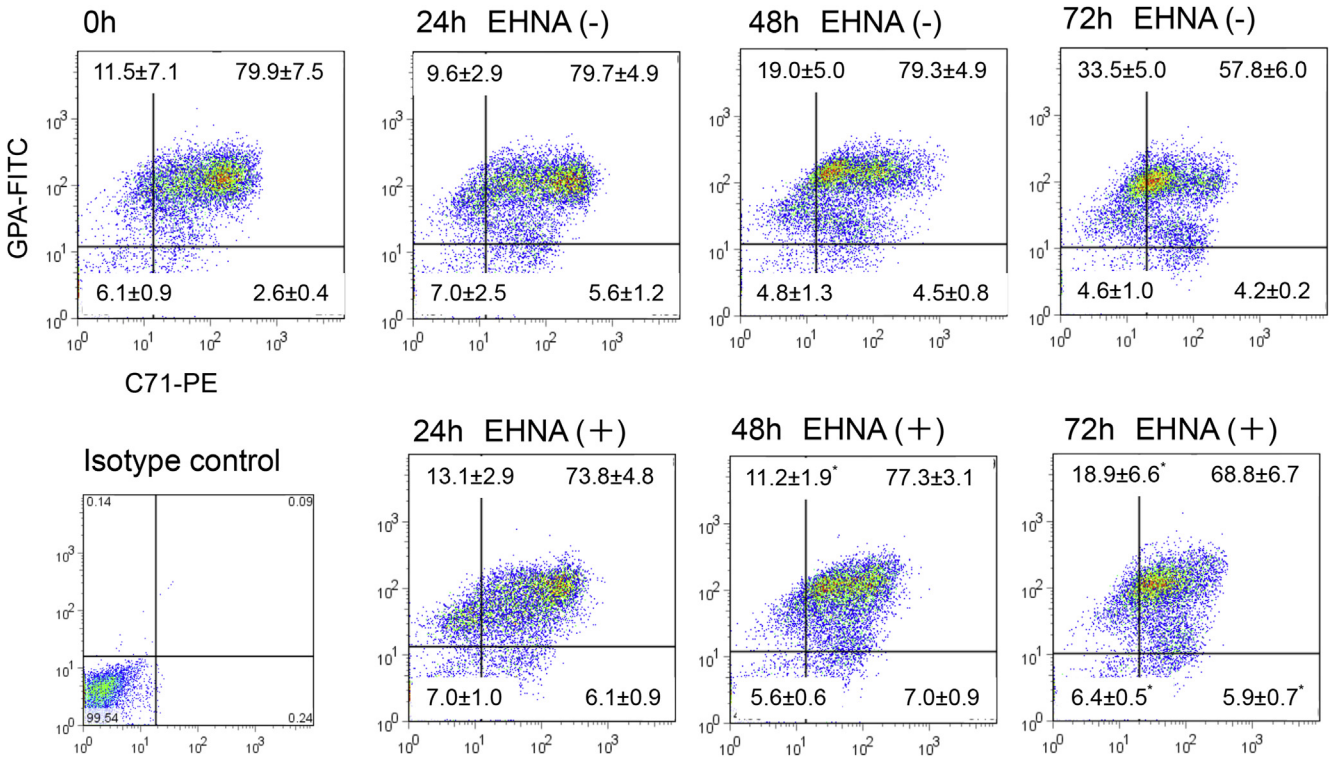

Supplementary Figure E7. To confirm the absence of a nonspecific effect of EHNA on protein expression, the D10 cell populations expressing CD71 and glycophorin A (GPA) in the presence and absence of EHNA (400 μmol/L) were analyzed using flow cytometry. After incubation for 48 hours in the presence of EHNA, the population of double-positive ($CD71^+$ and GPA^+) D10 cells was unchanged. By contrast, among those incubated in the absence of EHNA, the population of double-positive cells was increased. These results indicate that EHNA blocked enucleation of the D10 cells by inhibiting dynein.

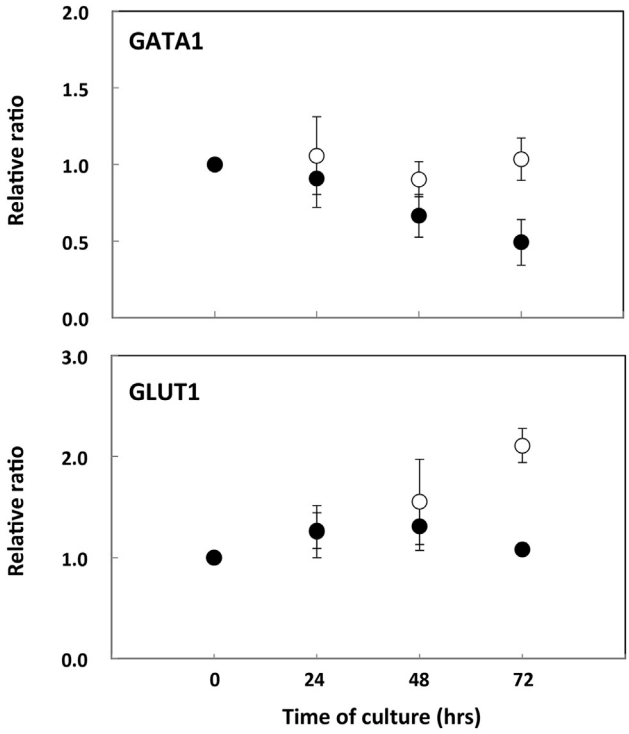

Supplementary Figure E8. Real-time RT-PCR of GATA1 and GLUT1 in D10 cells treated with (●) or without (○) EHNA is shown. Three independent experiments were performed, and the data are presented as the average and SE. After incubation of the cells with or without 400 μM EHNA for 24 hours, there were no significant differences in mRNA levels. After 72 hours, however, levels of both GATA1 and GLUT1 mRNA were reduced in D10 cells exposed to EHNA.

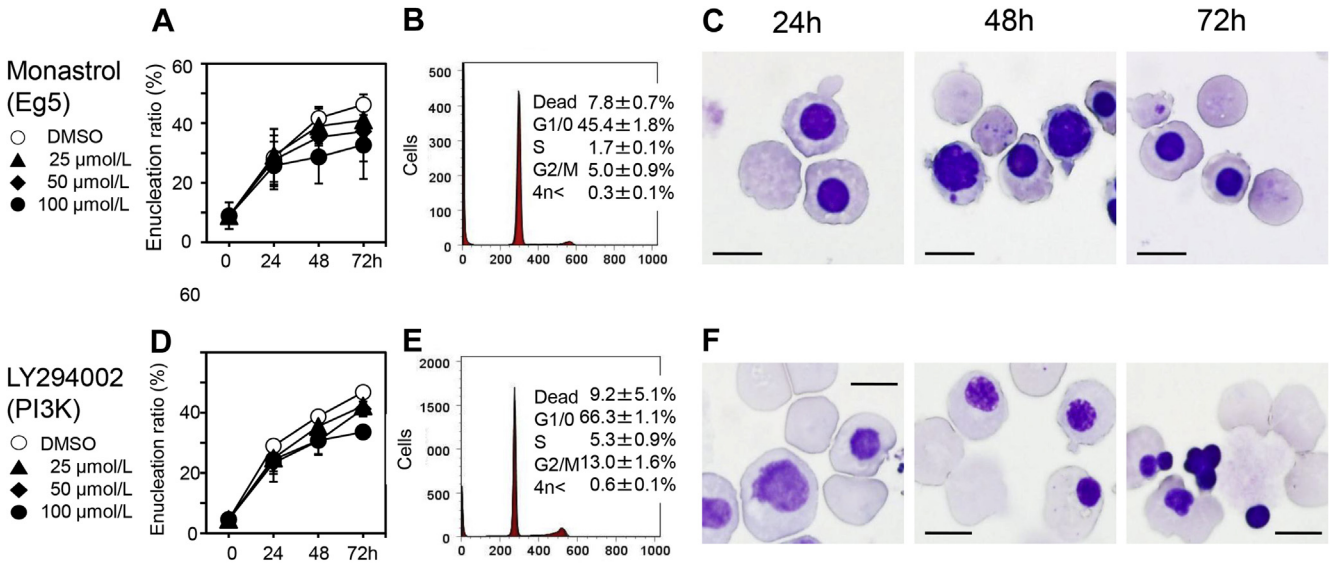

Supplementary Figure E9. D10 cells were cultured for 3 days in the presence of EPO with or without inhibitors Eg5 (monastrol, **A**–**C**) and PI3K (LY294002, **D**–**F**). (**A**, **D**) Effects of the indicated concentrations of inhibitors or vehicle on enucleation of D11–D13 erythroblasts. Results are presented as the means ± SD of three independent experiments. (**B**, **E**) Cell cycle analysis of D11 cells after culture for 24 hours with (*red lines*) or without (*black lines*) 100 μmol/L monastrol (**B**) and 100 μmol/L LY294002 (**E**). A representative result from three independent experiments is presented as the mean ± SD. (**C**, **F**) May–Grünwald–Giemsa staining of D11–D13 cells after culture for 24, 48, or 72 hours with or without 100 μmol/L monastrol (**C**) and 100 μmol/L LY294002 (**F**). A representative result from three independent experiments is shown. Bar = 10 μm.

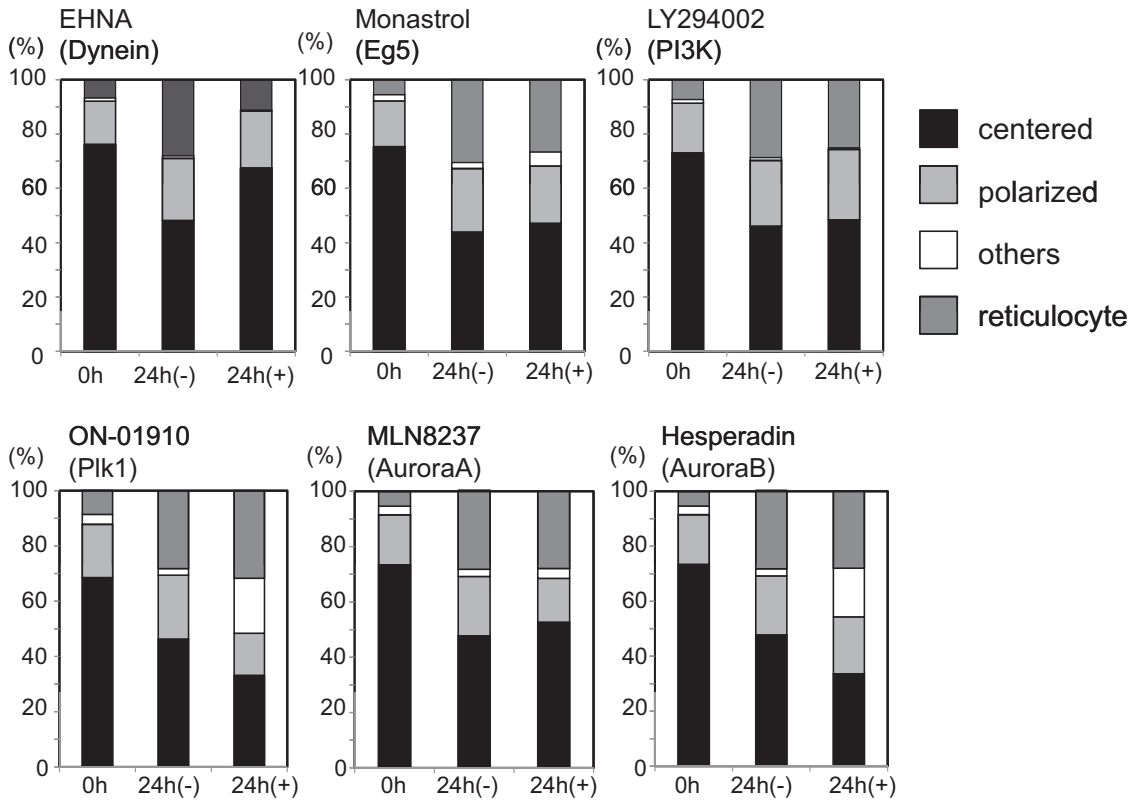

Supplementary Figure E10. Graphic presentation of the nuclear positioning in D10 cells incubated with inhibitors of the indicated proteins. Data are summarized in Table 1.

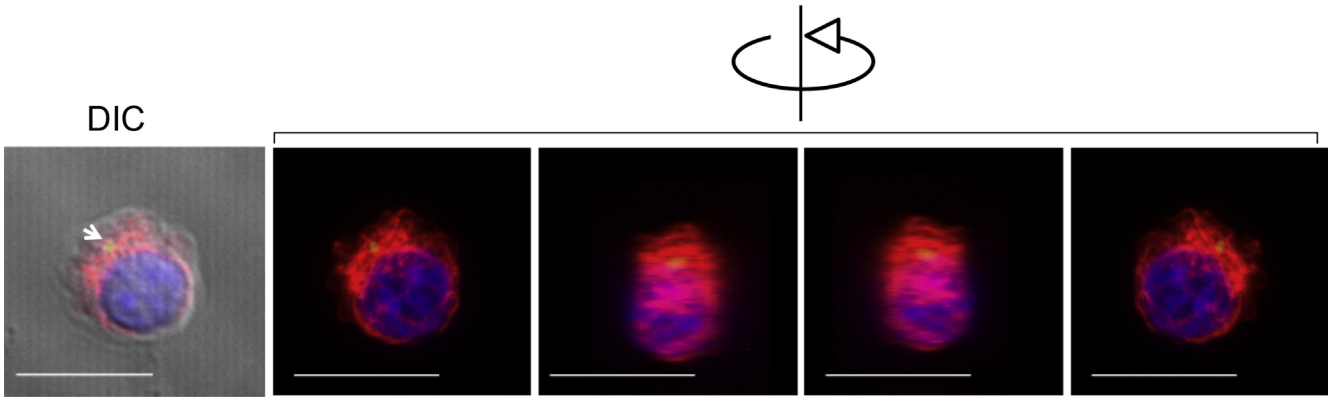

Supplementary Figure E11. Three-dimensional confocal micrographs of a D11 cell stained with anti-α-tubulin (*red*), anti-γ-tubulin (*green*, indicated by *arrow*). The differential interference contrast microscopic image (DIC) is labeled. Overlap of the α-tubulin and γ-tubulin staining is shown in *yellow* in the merged image (indicating by *arrowhead* in DIC image). Bar = 10 μm.

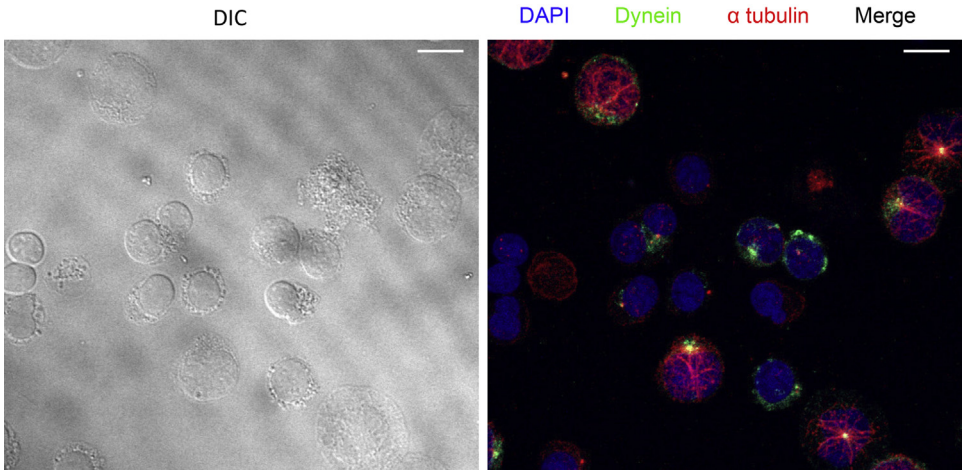

Supplementary Figure E12. Confocal micrographs of enucleating erythroblasts (D11) stained with DAPI (*blue*) and antibodies against dynein (*green*) and α-tubulin (*red*). The differential interference contrast microscopic image (DIC) is labeled. Overlap of the dynein and α-tubulin staining is shown in *yellow* in the merged image. Bar = 10 μm.

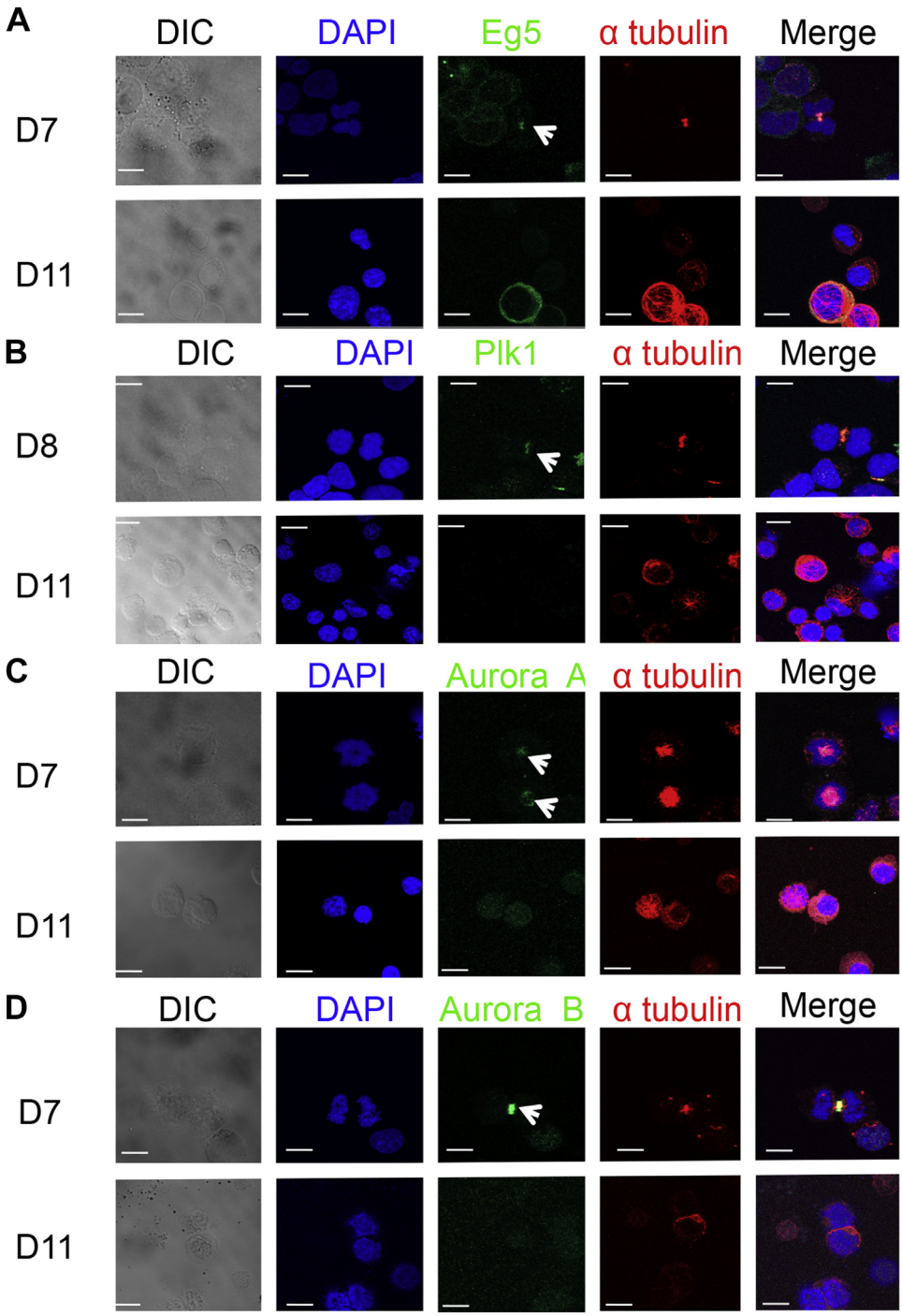

Supplementary Figure E13. Confocal micrographs of CFU-Es (D7 or D8) and enucleating erythroblasts (D11) stained with DAPI (*blue*) and antibodies against α-tubulin (*red*) plus antibodies against Eg5 (**A**), Plk1 (**B**), aurora A (**C**), or aurora B (**D**) (*green*, indicated by *arrowheads*). Overlap of the respective distributions is shown in *yellow* in the merged images. Bar = 10 μm.

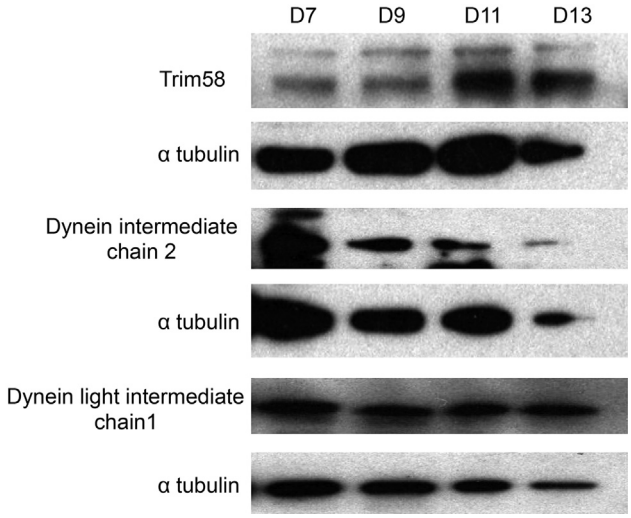

Supplementary Figure E14. Expression of Tim58 and dynein during erythropoiesis. Shown are Western blots of human CFU-Es (D7), erythroblasts (D9 and D11) and enucleated reticulocytes (D13). CFU-Es generated from purified $CD34^+$ cells were cultured for the indicated periods, after which cells were harvested, and protein from 1×10^5 cells was applied to each lane. Expression of α-tubulin, Teim58, dynein intermediate chain 2, and dynein light intermediate chain 1 was analyzed using specific antibodies against these antigens.